Subassemblage Cyclic Loading Test of RC Frame with Buckling Restrained Braces in Zigzag Configuration

Zhe Qu, Shoichi Kishiki, Hiroyasu Sakata, Akira Wada, Yusuke Maida

Abstract: A new buckling restrained braced frame system is proposed for reinforced concrete building structures, which is featured by the zigzag configuration of the braces and the corresponding connection details. The connection details tend to separate the vertical and horizontal components of force imposed by the braces to be resisted by independent structural components so as to make the behavior of the connection easier to estimate and control. The performance of the brace connection details was evaluated through cyclic load testing on 1/2-scale subassemblies of the proposed system, each of which consisted of a reinforced concrete part and a set of buckling restrained braces. In order to simplify the test control, the specimens were rotated ninety degrees in the test and were loaded by two displacement controlled actuators. The test results show that the normal and the shear resistance of the gusset plate connection are essentially independent of each other. However, the rotation of the gusset plate with respect to the beam-to-column joint may result in non-uniform force distribution of the anchor bolts, the primary resistance for tensile force. At the same time, such rotation may also subject the concrete corbels, the primary shear resistance, to unfavorable tensile force. In addition, it is also confirmed that the buckling restrained braces performed well in the proposed system.
Keywords: buckling restrained braced frame, reinforced concrete, subassemblage test

1 Introduction

Buckling restrained braces (BRBs), which exhibit stable hysteretic behavior and provide superior energy dissipation capacity to building structures, have been extensively studied and applied to various types of steel braced frames since 1980s [1, 2]. In contrast, however, the applications of BRBs in reinforced concrete (RC) structures are quite limited, and are mostly confined to the retrofit of existing buildings. In retrofitting RC buildings with BRBs, it is usually preferred either to attach some new frames to the outside of (e.g., [3]) or to insert individual internal braced steel frames to existing RC building (e.g., [4]) in order to avoid direct fastening of BRBs to existing concrete members. More direct and compact methods of fastening BRBs to RC structures were also tested, including fastening the gusset plates of BRBs to the side surface of the concrete beams by pre-stressing steel rods ([5, 6]), and, more straightforwardly, connecting the gusset plates through anchor bolts embedded in the concrete members (e.g., [7]).

For new RC constructions, the connection details for BRBs can be made with more options. Ogawa *et al.* [8] reported their test on V and inverted-V buckling restrained braced RC frames. A considerable amount of wide flange steel was embedded in the concrete members, primarily in the beams and the beam-to-column joints, to receive the BRB gusset plates. Gu *et al.* [9] also attempted to apply BRBs in newly-built RC frame buildings. In their method of connection, steel cages, each of which consisted of a top and a bottom plate that were welded with transverse steel rebars, were embedded at the end of the beams and the columns to receive the BRB gusset plates.

Analytical studies have also been conducted to evaluate the efficiency of BRBs in protecting RC buildings. Sarno and Manfredi [10] introduced their nonlinear static and dynamic analyses of a non-ductile RC frame building in Italy retrofitted by BRBs. Both V bracing and diagonal bracing systems were examined. Oviedo *et al.* [11] investigated the seismic performance of an example inverted-V braced RC frame building with BRBs through nonlinear dynamic analysis. A 'constant yield story drift ratio' criterion was proposed for proportioning BRBs in RC buildings.

Despite the various details of BRB connection and the neglect of the influence of BRB connection in the analysis, all above studies reported good performance of BRBs to dissipate energy and to enhance the seismic performance of RC frames. However, searching for appropriate methods of applying BRBs in RC frame buildings remains an important issue for RC construction, and is especially interesting for the applications in new construction because it is more flexible for developing innovative buckling restrained braced systems to better accommodate BRBs in RC buildings.

The existence of a BRB gusset plate may subject the surrounding concrete members to very complicated, and sometimes unfavorable, load conditions. The damage of the surrounding concrete may, in turn, impair the performance of the BRB connection. In addition, the BRBs, which carry significant axial force, are likely to change the force distribution of its surrounding frame members. For example, considerable axial tensile force may be transmitted by the BRBs to the RC columns in the braced span, which may even exceed the gravity load and subject the columns to tension. As an attempt to address some of the above issues, a new bracing system of BRBs in a zigzag configuration, which is referred to as 'continuously buckling restrained braced frame' (CBRBF) system herein, and corresponding details of the BRB connection are proposed for RC buildings. In this system, the BRBs are arranged continuously along the height of the braced span and the two BRBs in adjacent stories share the same gusset plate, which is attached to the surface of the concrete beam-to-column joint. This is made possible by abandoning the beams in the braced span (see the 'braced frame' in Figure 1(a) for example). In such a manner, the braced span forms a structure like a Warren truss. As can be seen in Figure 1(a), the braced frame is connected with the rest of the structure through the floor system, which consists of floor slabs, two way beams and secondary beams if necessary.

The proposed connection for BRB gusset plate consists of a set of pre-stressing bolts to transmit the tensile component and a pair of RC corbels to transmit the shear component of the force in BRBs (Figure 1(b)). In such a manner, the horizontal and the vertical resistance of the connection are expected to be separated so that the pre-stressing bolts are responsible for only the horizontal component of the BRB force and the corbels the vertical one. As a result, both the pre-stressing bolts and the corbels are under relatively simple load conditions and their behavior becomes easier to predict and control. An additional benefit of attaching the gusset plate to the side of the beam-to-column joint, rather than to the column ends, is that the impairment of the column slenderness and thus the potential of unfavorable shear failure of a captive column can be reduced.

In order to validate of the proposed connection details, cyclic loading test on 1/2-scale subassemblies of CBRBF system was conducted. Insight into the local behavior of the proposed braced RC frame system and that of the BRB connection was obtained.

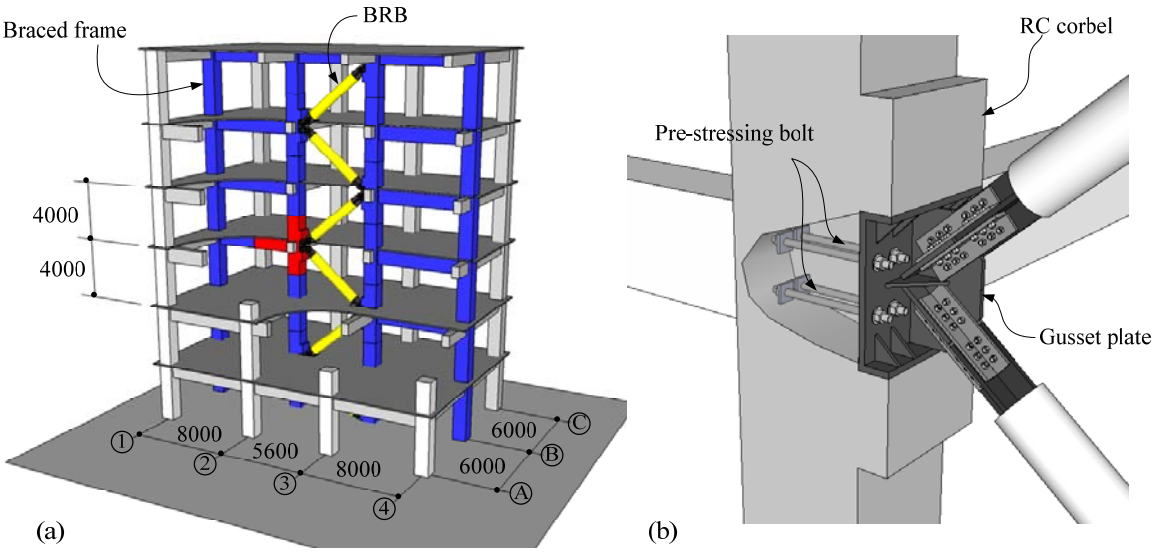

Figure 1. RC continuously buckling restrained braced frame: (a) structural layout and BRB configuration and (b) details of BRB connection.

2 Experimental program

2.1 Specimens

Figure 1(a) shows an archetype CBRBF system. The subassemblage, which is colored in red, is separated from the rest of the structure by assuming that the inflection points of both the beam and the column are located at the center of their length, and its 1/2-scale model was taken as the test specimen. The RC part of the specimen consisted of a column extending half the story height above and below the joint, and a half-span beam framing into it. The dimensions and reinforcement of the RC part of the scaled specimens are given in Figure 2.

The RC part was detailed in accordance with the latest AIJ standard for concrete structures [12]. The column had a square cross section of 450 mm by 450 mm. It was reinforced by 16 ϕ19 longitudinal rebars, resulting in 2.3% gross reinforcement ratio, and ϕ6 triple hoops at 50 mm spacing, resulting in 0.85% transverse reinforcement ratio. The beam cross section was 450 mm in height and 275 mm in width. It was symmetrically reinforced by 12 ϕ19 longitudinal rebars, 1.6% reinforcement ratio for bending. ϕ6 closed double stirrups were placed at 90 mm interval within the 450 mm range close to the beam end and at 150 mm interval in the rest part of the beam. The transverse reinforcement ratio is 0.52% and 0.31% in these two ranges, respectively.

The gravity axial compressive force in the column was exerted by means of six unbonded pre-stressing steel rods passing through the center portion of the column. A total of about 1000 kN axial compressive force was provided by the pre-stressing force, resulting in an axial force ratio of about 0.1.

A pair of reinforced concrete corbels, 450 mm in depth and 70 mm in length, projected from the column to hold the gusset plate. The corbels were reinforced by ϕ10 U-shape double stirrups at 50 mm spacing (see Section B in Figure 2). As predicted by a strut-and-tie model proposed by Qu et al (2012) [13], the shear strength of such a corbel was about 1100 kN. To eliminate the initial gap between the gusset plate and the corbels, high-strength non-shrink grout was injected into the preserved 10 mm gap for both corbels after the gusset plate was

properly fastened. Eight ϕ17 high-strength pre-stressing bolts were embedded in the RC beam-to-column joint to fasten the gusset plate.

Ideally, the two BRBs connecting to the same gusset plate in a CBRBF system may yield at the same time and in opposite directions (i.e., one in tension and the other in compression) so that the horizontal components of their force can counter-act each other and thus impose very small demand for the pre-stressing bolts. However, significant tensile force in the pre-stressing bolts may arise from the higher mode vibration of the system especially after the BRB yield and the 1st mode vibration is greatly suppressed. Some other sources may also contribute to this tensile force demand. For example, the difference in strength of the two BRBs in the neighboring stories, and the circumstances for the top story where there is only a single BRB.

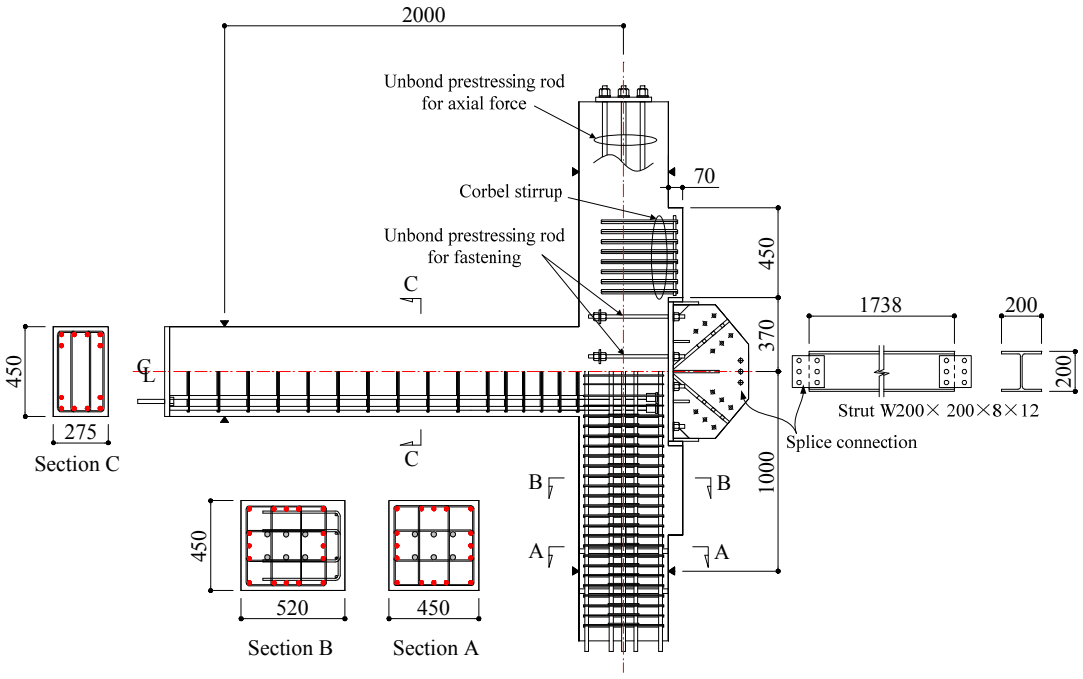

Figure 2. Reinforced concrete part of specimen with gusset plate installed and the strut.

In order to simulate this tensile force demand for the pre-stressing bolts in the static test, subassemblies with different proportions of yield strength of the two BRBs were tested (Table 1). When identical BRBs are used in both the lower and the upper stories, for example, in Specimen No.1, the gusset plate is not likely to be subject to considerable tensile force. For Specimen No.2, BRBs with different yield strength, that is, 750 kN for the lower and 500 kN for the upper story, were used. For Specimen No. 3 and No. 4, only a single BRB of 750 kN was installed in the lower story to impose even greater tensile force on the gusset plate.

The pre-stressing bolts for fastening the gusset plate were designed to be pre-stressed to a total of 571.2 kN for the first three specimens, which is equal to the horizontal component of the yield strength of a single 750kN BRB. The actual pre-stressing force was, however, somewhat lower than the design value for all the three specimens according to the strain readings of the gages on the bolts (Table 1). For Specimen No.4, the bolts were fastened by hand and no pre-tensioning was conducted. Instead, a horizontal strut, made of wide flange steel W200×200×8×12, was installed between the gusset plate and the column on the other

side of the span, that is, in the position of the eliminated beam, to help carrying the tensile force on the gusset plate. Flexible bolt connections were provided at both ends of the strut to suppress transmission of moment.

Table 1. BRB arrangement and gusset plate fastening.

	No. 1	No. 2	No. 3	No. 4
Nominal yield strength of upper BRB (kN)	750	500	0	0
Nominal yield strength of lower BRB (kN)	750	750	750	750
Design pre-stressing force, P_{0d} (kN)	571.2	571.2	571.2	0
Actual pre-stressing force, P_0 (kN)	504.1	515.0	511.5	0
With or without a strut	w/o	w/o	w/o	w/

All the specimens were cast with a single batch of concrete, 50 MPa nominal compressive strength. The properties of concrete and the grout for each specimen, including the compressive strength, f_c', split tensile strength, f_{ts}, and elastic modulus, E_c, were tested on the day of loading (see Table 2). For the steel rebars, the measured yield strength, f_y, ultimate strength, f_u and elastic modulus, E_s are listed in Table 3, together with their nominal yield strength, f_{yn}. With the nominal strength of concrete and steel, the flexural strength of the column is about 1.37 times that of the beam if the axial force in the column is neglected. With 1000 kN initial axial force in the column, this ratio rises to 1.88, a pretty high ratio to demonstrate the 'strong column-weak beam' concept for RC moment-resisting frames.

For all the BRBs used in the test, steel tubes filled with mortar were used to restrain the buckling of the steel core. For both the 750 kN and the 500 kN BRBs, the overall length was 2278 mm and the length of the plastic segment was 1262 mm. The elastic segment had a cruciform cross section and the plastic segment was simply a flat plate 16 mm in thickness (Figure 3). LY225 steel, which is widely used for hysteretic energy dissipating devices in Japan, was used for the core. Its measured properties are also given in Table 3.

Table 2. Material properties of concrete and grout.

	Concrete			Grout	
	f_c' (MPa)	f_{ts} (MPa)	E_c (GPa)	f_c' (MPa)	E_c (GPa)
No.1(4/25)	68.2	3.67	31.4	86.5	33.7
No.2(5/17)	68.9	3.57	31.4	95.2	33.6
No.3(5/11)	65.8	3.96	31.5	94.6	32.8
No.4(5/25)	71.4	4.32	32.6	103	31.8

Table 3. Material properties of steel.

	f_{yn} (MPa)	f_y (MPa)	f_u (MPa)	E_s (GPa)
Longitudinal rebar, D19 (SD490)	490	528	737	190
Column and beam stirrup, U6 (USD685)	685	693	914	191
Corbel stirrup, D10 (SD295A)	295	366	520	203
BRB core (LY225)	225	210	302	203

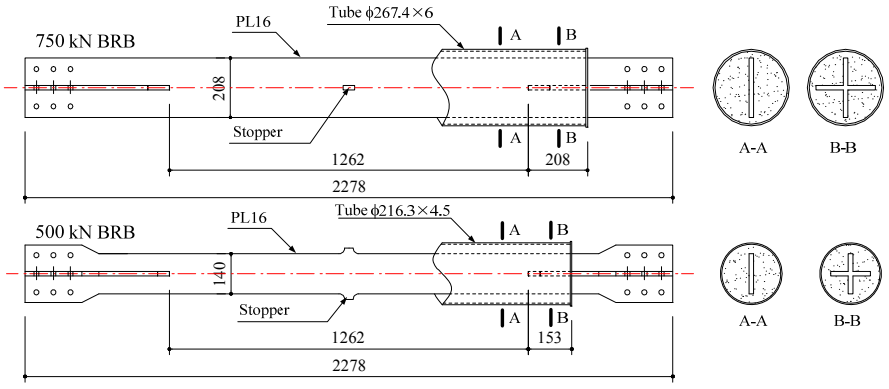

Figure 3. Buckling restrained braces.

2.2 Loading setup

Taking two stories out of the 1/2-scale archetype CBRBF system, its deformed shape under lateral force can be readily obtained, as shown in Figure 4(a), assuming that the inflection points of the beams and the columns are located at their centers and neglecting their axial deformation induced by the lateral force. It is also assumed that story drift ratios of the lower and the upper story are the same so that the three beam-to-column joints on the same column (e.g., those at point O, P and Q) lie on the same straight line. Given the story drift ratio θ, such lateral deformations can also be regarded as a consequence of the movement of the left hand side frame along a circular orbit by an angle of θ with respect to the right hand side frame. For example, the point A and B in the left hand side frame move along a circular orbit (i.e., B-B' and A-A') around the point O in the right hand side frame to A' and B', keeping the span length unchanged. The relative movement of A and B parallel with the centerline of the column with respect to O are δ_c and $\delta_c + \delta_b$, respectively (Figure 4(a)). Note that OB may not keep perpendicular to the deformed column because of the rotation of the joint (e.g., at O and A'). Instead, it is perpendicular to the straight line connecting the joints on the same column, that is, line PQ, the dashed line in Figure 4. The rotating angle of the left-hand frame, which inherently equals to the story drift ratio, θ, based on the above assumptions, should not be mistaken as the rotation of the beam-to-column joint.

Regarding the subassemblage to be tested, it is easier to reproduce physically such deformations if the subassembly is rotated 90 degrees clockwise considering the limitation of available testing facilities. In the rotated version (Figure 4(b)), the two assumed inflection points of the column (point C and D) and that of the beam (point B) are constrained to move only along circular orbits and thus the subassemblage need only be driven by two actuators horizontally, one on the column end to deform the BRBs and the other on the beam end (point B) to deform the concrete part.

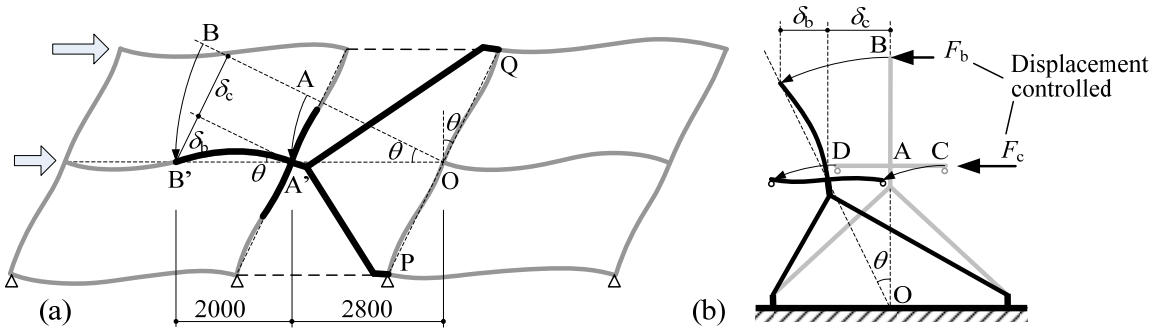

Figure 4. Deformed shape of subassemblage.

Necessary boundary conditions were accomplished through the setup shown in Figure 5. The pin points on the column (C and D in Figure 4(b)) were fastened to steel beams, each of which was constrained by a pair of wide flange steel swaying posts with pins at both ends to exhibit only circular motion. Pin load cells were used for the lower pins of the four swaying posts to obtain the shear force in the column. The beam end (point B in Figure 4(b)) was also constrained to exhibit circular motion by a pair of extended actuators with pins at both ends. The displacement of these actuators were kept zero during the test. The column was driven by a 2000 kN displacement-controlled actuator to deform the BRBs and the beam was driven by a 1000 kN displacement-controlled actuator to deform the frame part. Cyclic loading with increasing story drift amplitudes was conducted for each specimen. The sequence of loading amplitudes and the number of loading cycles are listed in Table 4. Loading towards the left hand side of the rotated specimen as shown in Figure 5 was taken as positive.

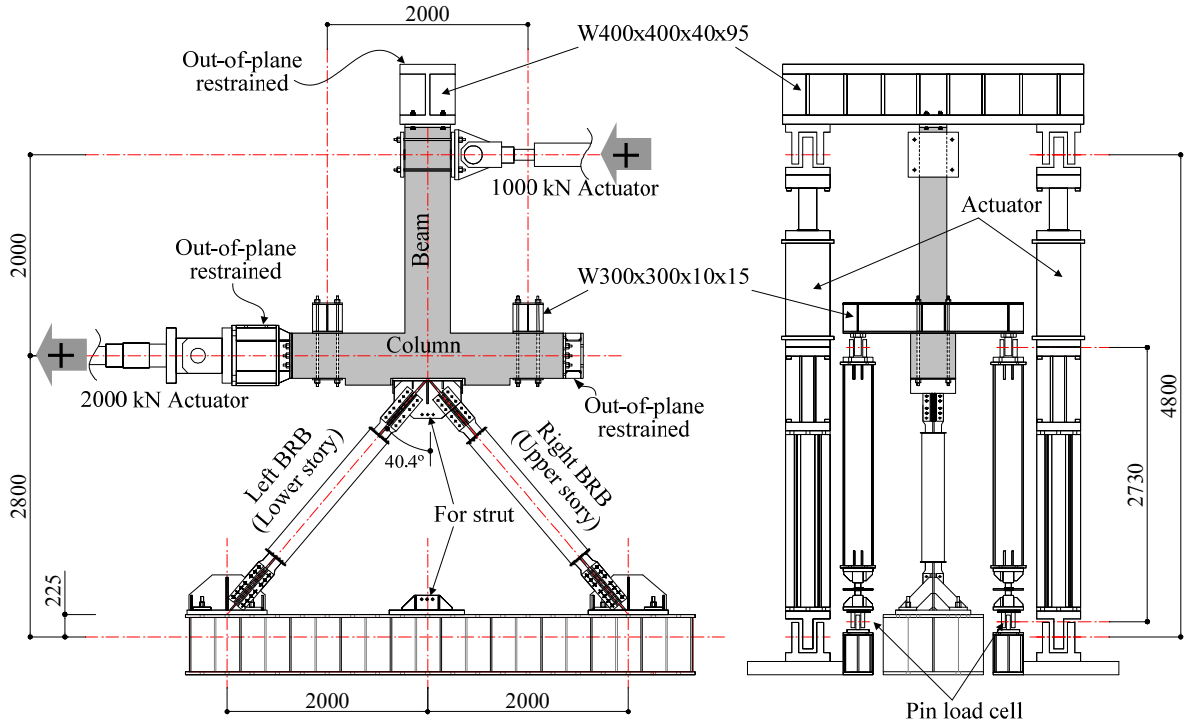

Figure 5. Test setup.

In the prescribed loading history, the 1/1600 load cycles serve as pre-load tests to verify the loading control system. The behavior of the specimen before the BRBs yield are to be confirmed in the 1/800 load cycles because it was estimated that the 750 kN BRBs would

yield at around 1/780 story drift ratio if all the parts are rigidly connected. 1/200 story drift ratio is the 'damage limit-state' deformation stipulated in the building codes of Japan [14]. 1/100 and 1/50 story drift ratios generally correspond to the 'ultimate limit-state' of passive-controlled buildings (those protected by specific energy dissipating devices) and conventional RC moment-resisting frame buildings, respectively [15].

Table 4 Loading history.

Story drift ratio amplitude	1/1600	1/800	1/400	1/200	1/100	1/50	1/33
Number of cycles	2	2	2	2	2	1	1

3 Test results and discussions for reinforced concrete part

The force equilibrium of the RC part of the specimen during positive loading is depicted in Figure 6. Note that the work point of the two BRBs was at the surface rather than the center of the column. As a result, the vertical component of the force in the gusset plate, V_{GP}, has contributed to the moment resisting capacity of the RC part by $V_{GP} \cdot h/2$, where h = 450 mm, is the height of the column section. Although the arm was short, the great force in the BRBs was able to make the resultant moment contribution comparable to that of the beam, thus to compensate some of the loss in the moment resisting capacity because of the elimination of the beam in the braced span. Figure 7 compares the total moment resisting capacity of the RC part, which is taken as $(V_{c1} + V_{c2}) \cdot H/2$, with the contribution of the beam, $V_b \cdot L_b/2$, and that of the BRBs, $V_{GP} \cdot h/2$, for Specimen No.2 for example, where H = 2000 mm, is the story height of the 1/2-scale specimen and L_b = 4000 mm, is the un-braced span length. In this case, the maximum moment contribution of the BRBs was about half that of the beam, that is, about one third of the total moment resisting capacity of the RC part.

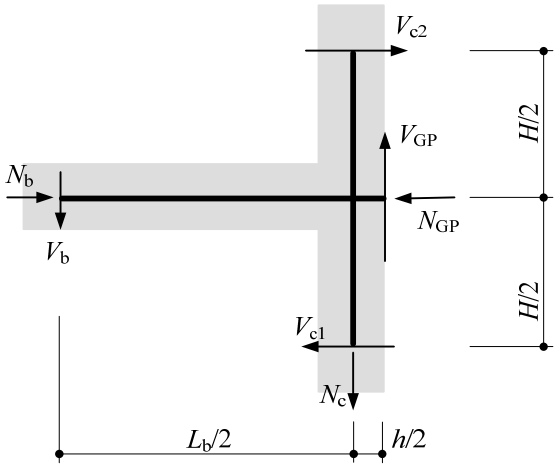

Figure 6. Force equilibrium of RC part.

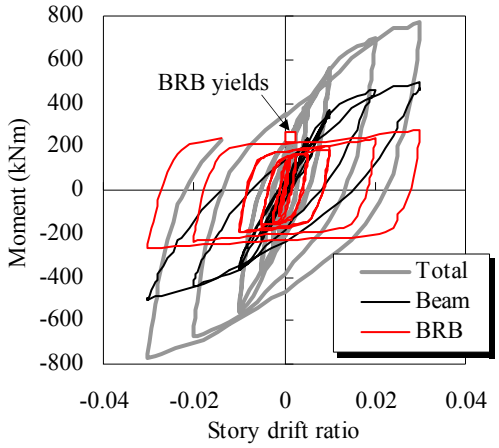

Figure 7. Moment resisting capacity of RC part in Specimen No.2.

For Specimen No.2, the BRBs yielded at an early stage of about 1/600 story drift ratio, when considerable cracking or other kinds of damage of the RC part could hardly be observed. In other words, the BRBs would begin to dissipate earthquake energy through plastic deformation before the RC part of the system sustains any considerable damage. Similar observations were made for all other specimens. The BRBs generally yielded at about

1/600 to 1/500 story drift ratio.

The vertical force imposed by the BRBs on the gusset plate, V_{GP}, was transmitted to the column by the RC corbels projecting from the column. This force may have changed the damage pattern of the column by reducing the bending moment in the column segment underneath the active corbel, that is, the corbel carrying the shear force. Figure 8 shows the cracks of the RC part during positive (Figure 8(a)) and negative loading (Figure 8(b)) at 1/50 story drift ratio. The flexural-shear cracks of the column appeared only in the lower half of the column during positive loads (Figure 8(a)) and only in the upper half of the column during negative loads (Figure 8(b)). In other words, the part of the column underneath the active corbel was free of flexural cracking. By looking into the strain of the longitudinal rebars, ε_s, which is also shown in Figure 8, it is found that the curvature of the column sections indicated by the strains agreed well with the observed cracking of the column. Both of them suggested that the column underneath the active corbel was subject to much less moment than the other half.

Besides, the shear force, V_{GP}, had an effect on the axial force in the column of the lower story. In particular, it subjected the part of the column lower than the active corbel to an additional tensile force under positive loads. Although this tensile force did not exceed the initial compressive force in the column, it decreased the flexural strength and cracking moment of the column and made it more vulnerable to cracking. Take Specimen No.2 for example. It can be seen that the flexural-shear cracks of the lower half column and the joint at +1/50 story drift ratio (Figure 8(a)) was more than those of the upper half column and the joint at -1/50 story drift ratio (Figure 8(b)).

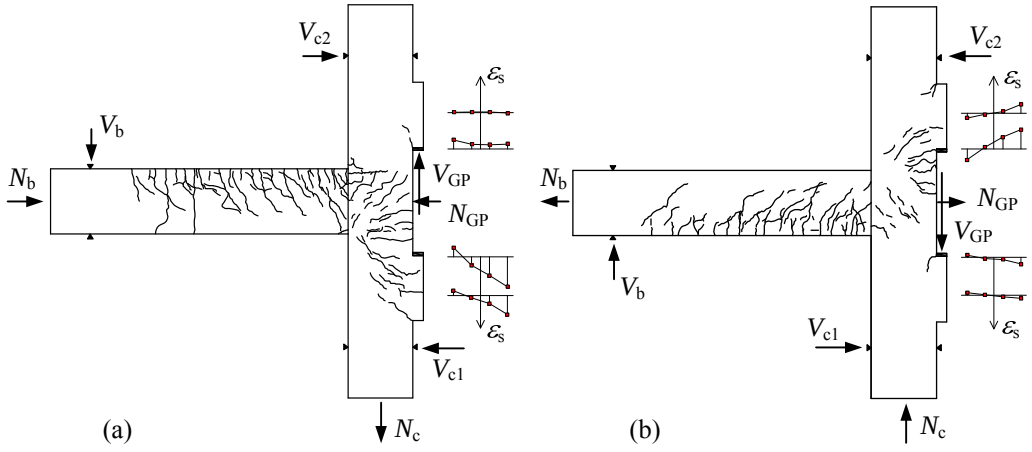

Figure 8. Cracks and strain of column longitudinal rebars of Specimen No.2 at: (a) +1/50 and (b) -1/50 story drift ratio.

4. Test results and discussions for buckling restrained braces

The load condition of buckling restrained braces (BRB) in a building structure or in subassemblage test may differ somewhat from that in a component test where the BRBs are subjected to only uniaxial load. One obvious difference is the rotation at the ends of a BRB when it is splice-connected to the gusset plate. The splice connection may transmit some moment to the brace as a result of the rotation of the frame joints, and the amount of such moment transmitted to the brace is limited by the forming of plastic hinges at both ends of the BRB. So far as the setup of the present test is concerned, the rotation at these plastic hinges,

denoted as θ_B, can be decomposed into two parts: (1) that because of the translation of the beam-to-column joint of the RC part, δ_c, (Figure 9(b)), denoted as θ_{B1}; and (2) that because of the rotation of the joint, θ_j, as shown in (Figure 9(c)), denoted as θ_{B2}. The superposition of the translational and rotational motion of the beam-to-column joint gives its total motion. Accordingly, the BRB end rotation, θ_B, is necessarily equal to the superposition of θ_{B1} and θ_{B2}, assuming that the gusset plate is rigid and is rigidly fastened to the RC joint and that the BRB segments outside the plastic hinges are also rigid.

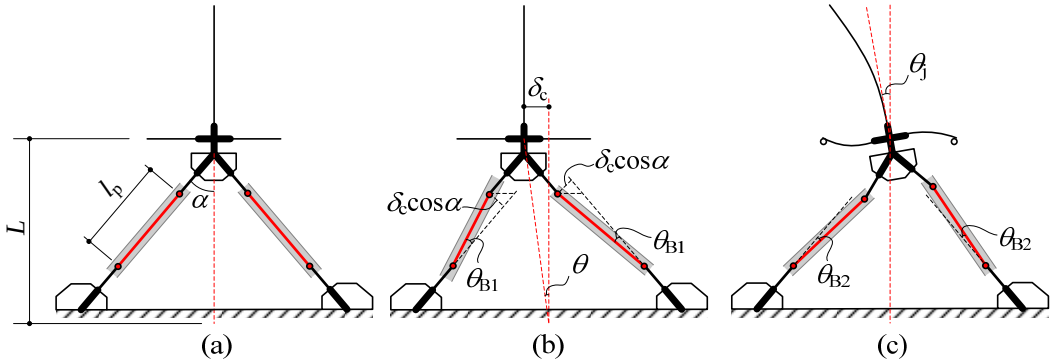

Figure 9. Mechanism of bending of BRBs: (a) undeformed shape, (b) deformation because of beam-to-column joint translation and (c) deformation because of beam-to-column joint rotation.

For the present test setup, the translation of the RC joint, δ_c, was directly related with the story drift ratio, θ, by $\delta_c = L\theta$, where L = 2800 mm, is the length of the braced span. The BRB end rotation because of the joint translation, θ_{B1}, can thus be readily related to the story drift ratio, θ, by Equation (1).

$$\theta_{B1} = \frac{L\cos\alpha}{l_p}\theta \tag{1}$$

where α = 40.4°, is the inclination angle of the BRBs, see Figure 9(a); l_p is the distance between the two plastic hinges at the ends of the BRB. Assuming that the plastic hinges form at the ends of the plastic segment of the core, l_p equals the length of the plastic segment, which was 1262 mm for both 750 kN and 500 kN BRB in the test.

The BRB end rotations were measured in the test by means of a pair of displacement transducers at each end of the BRB as shown in Figure 10. The clockwise rotation of the elastic segment with respect to the plastic one is taken as positive. This definition makes the rotation because of joint translation, θ_{B1}, bears the same sign as the story drift ratio, θ.

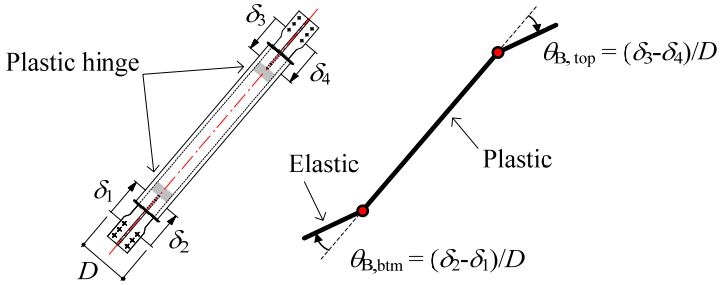

Figure 10. Measurement of BRB end rotation

The BRB end rotations in Specimen No.1, where two 750 kN BRBs were connected to the frame, and in Specimen No.3, where only a single 750 kN BRB was installed, are compared in Figure 11. Only the results for the left BRB, that is, the BRB in the lower story, of Specimen No.1 are shown in the graph and those of the other BRB were similar. θ_{B1} calculated by Equation (1) is also depicted in the graphs as bold straight lines for comparison. In both cases, $\theta_{B1} = 1.69\theta$. It is seen in Figure 11 that the measured BRB end rotation, θ_B, is less than the calculated θ_{B1} and may, quite accidentally, be better described by $\theta_B = \theta$. This was primarily attributed to the influence of θ_{B2}, which always tended to reduce the BRB end rotation, as it is always in the opposite direction as θ_{B1}. The observed BRB end rotations reported by Tsai and Hisao (2008) [16] were also plotted in Figure 11(a) for comparison. They were measured during a series of pseudo dynamic tests on a full-scale three-story inverted-V buckling restrained braced frame with steel beams and concrete filled tube columns. It seems that the BRB end rotations in the CBRBF subassemblies in the present test were similar to those measured at the top ends and were much greater than those measured at the bottom ends of the BRBs in the inverted-V braced frame.

Despite the obvious rotations at the ends, all of the BRBs exhibited hysteresis practically the same as that in a uniaxial component test, which was carried out on a 750 kN BRB before the subassemblage test (Figure 12). The BRBs in the subassemblage test exhibited greater strength in compression than in tension, a consequence of the increased friction between the core and the restraining tube by the Poisson effect and possibly the local buckling of the core. It has little to do with the plastic rotations at the BRB ends because similar phenomenon was also observed in the component test where BRB end rotations were negligible (Figure 12(c)).

Note that the different strength of a BRB in compression and in tension, as observed in the test, may introduce some normal force to the gusset plate even if identical BRBs are used in the lower and the upper stories. However, the thus-induced normal force always tends to push the gusset plate against the RC joint, thus causes no problem for the anchor bolts.

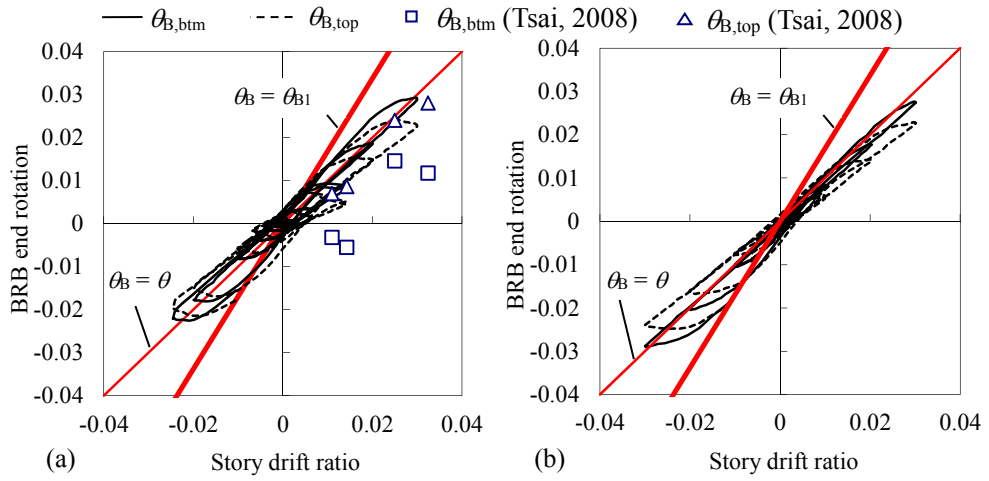

Figure 11. Measured end rotations of 750 kN left BRB (lower story) in (a) Specimen No.1 and (b) Specimen No.3.

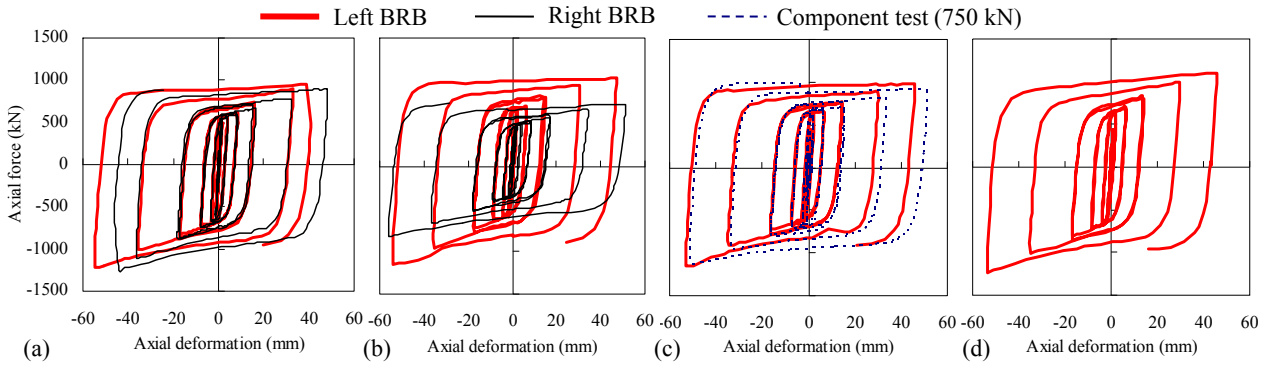

Figure 12. BRB hysteresis: (a) Specimen No.1, (b) No.2, (c) No.3 and (d) No.4.

5. Test results and discussions for BRB connection

The BRB connection includes both the connection of the brace to the gusset plate and that of the gusset plate to the RC part. In the present test, the former was simply a splice connection that is commonly used for BRBs in practical construction. These splice connections worked well and remained essentially elastic during the test. The gusset plate too, well stiffened by ribs, worked well and sustained no buckling or yielding in the test. In the following discussions, attention will be given to the connection of the gusset plate to the RC part. As mentioned above, the gusset plate was fastened to the RC beam-to-column joint by pre-stressing bolts embedded in the joint and was held by a pair of RC corbels projecting from the column. Ideally, the pre-stressing bolts that provide the resistance normal to the column surface and the RC corbels that provide shear resistance are expected to be independent of each other, and also be independent of the behavior of the RC column. In the test, however, some interdependence was observed.

5.1 Normal response

In the test, the gusset plate was always pushed against the RC joint when the specimen was loaded towards the positive direction, and was pulled away from the joint in negative loading (except for Specimen No.1). Compared with the compressive behavior, the tensile behavior normal to the RC joint surface is of much greater importance and interest for the current details. Figure 13 shows the force equilibrium of the gusset plate during negative loading for specimens without a strut (No.3) (Figure 13(a)) and for the specimen with a strut (No.4) (Figure 13(b)). The resultant BRB force in the normal direction tends to pull the gusset plate away from the joint, especially for Specimen No.3 and No.4 because there was no BRB installed in the upper story, that is, $F_{BRB,U}$ was zero. At the same time, the lower toe of the gusset plate was tightly compressed against the lower RC corbel in consequence of the great vertical resultant force of the BRB. As a result, the friction force, N_{corbel}, between the lower toe of the gusset plate and the RC corbel may increase and join the pre-stressing bolts in preventing the gusset plate from being pulled out and thus may lead to clockwise rotation of the gusset plate. This rotation was confirmed by the measured deformation of the four rows of pre-stressing bolts. A pair of strain gages was attached at the center of each bolt as shown in Figure 13. The average of the readings of the two gages multiplied by the length of the bolt was taken as the deformation of the bolt. The bolt deformation at various negative peak story drift ratios is depicted in Figure 14.

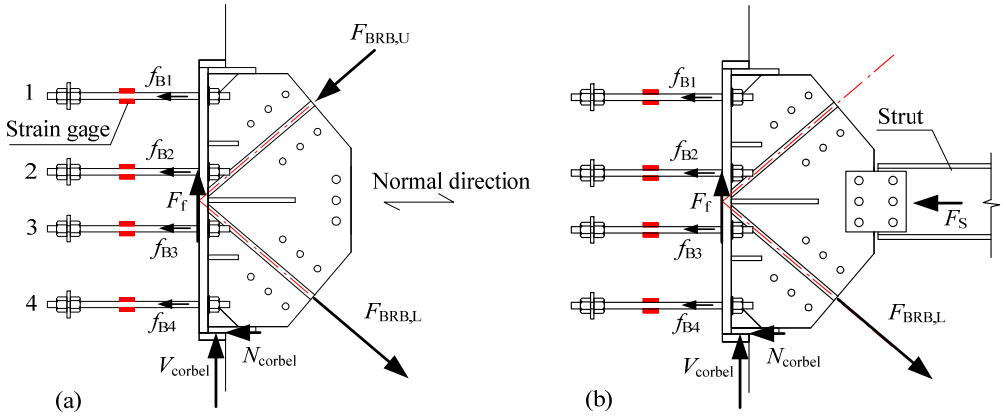

Figure 13. Force equilibrium of gusset plate during negative loading and measurement of bolt deformation: (a) Specimen No.3 and (b) No.4.

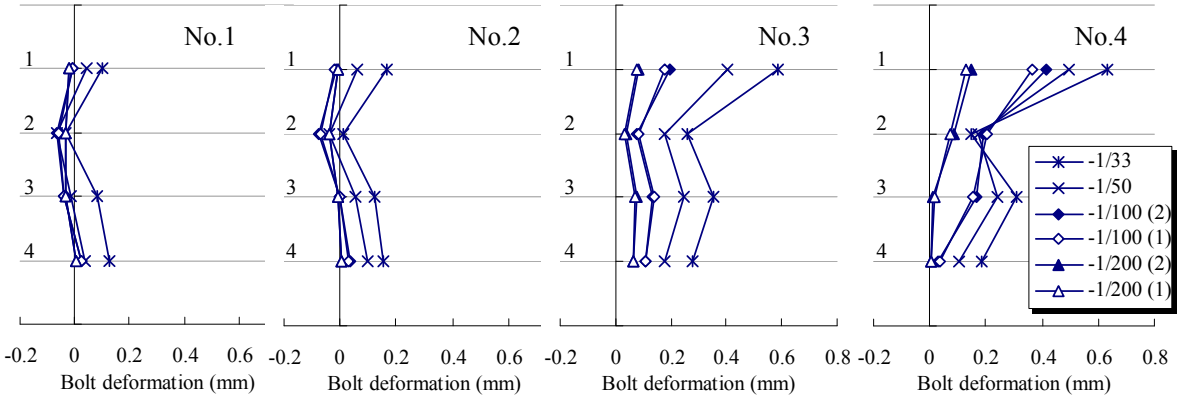

Figure 14. Bolt deformation.

For Specimen No.3 and No.4, the clockwise rotation of the gusset plate was evident. It is also worth noting that, notwithstanding the existence of a strut, the rotation of the gusset plate in Specimen No.4 seems to be even greater than that in Specimen No.3. Such rotation, which was primarily the result of the friction force, N_{corbel}, may make the tensile force in the upper bolts much greater than that in the lower ones, thus may lead to greater demand for ensuring the bolt group to remain elastic. In addition, the friction between the gusset plate and the RC corbel would subject the corbel to tensile force, which would degrade its shear strength. In order to avoid the unevenly distributed force in the bolts and the degradation of the corbel shear strength because of tensile force, it would be preferable to minimize the friction between the gusset plate and the RC corbel, for example, by using some Teflon cushion.

For an unbonded pre-stressing bolt embedded in a concrete block and subjected to tensile force (Figure 15(a)), its force-displacement relationship may be idealized by a tri-linear curve, which features a separation point before the yield of the bolt (Figure 15(b)). Before the separation, the embedded pre-stressing bolt can be treated as two springs in parallel, a bolt spring representing the bolt itself, and a concrete spring representing the surrounding concrete between the anchor plate and the base plate. It may thus exhibit very large stiffness because of the large axial stiffness of the concrete spring. When the tensile force exceeds a certain limit, which is usually a little bit greater than the initial pre-stressing force P_0 in the bolt, the base plate may separate from the concrete surface. After the separation, the embedded bolt can be treated as the above two springs in series. Accordingly, the post-separation stiffness becomes much less than that before the separation. When the

gusset plate is gradually pulled away from the underneath concrete, the compressive force on the concrete surface is gradually released and thus the load condition of the underneath concrete keeps changing. This may change the stiffness of the representative concrete spring. However, it is practically acceptable to assume the stiffness of the concrete spring to be constant because it is generally several times greater than the stiffness of the bolt spring and it is usually subjected to considerable uncertainty.

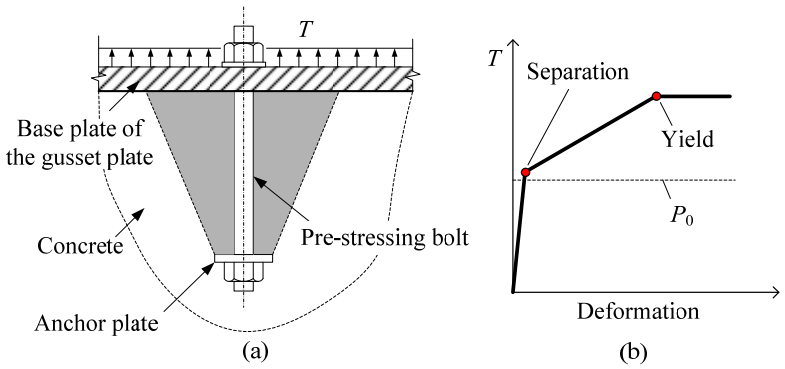

Figure 15. (a) Embedded pre-stressing bolt subjected to tension and (b) idealized tensile force-deformation relationship.

As a result of the different initial pre-stressing force, P_0, the bolts in Specimen No.3 and No.4 in the subassemblage test behaved quite differently. The force-displacement relationship of the gusset plates in the two specimens are shown in Figure 16. Recall the force equilibrium in Figure 6. The force of the gusset plate in the normal direction, N_{GP}, can be obtained by summing up the beam axial force, N_b, and the column shear force, V_{c1} and V_{c2}, which were recorded by load cells in the test. The normal displacement of the gusset plate is taken as the average deformation of the bolt deformation, which was calculated by the above-mentioned strain readings.

The nominal yield strength of the bolt group (i.e., 8ϕ17 SBPR 1080/1230) in the test was no less than 1968 kN, so much greater than the expected tensile force that no yielding of the bolts should be expected even if the above-mentioned unevenly distributed force in the bolts is taken into account. The initial pre-stressing force for Specimen No.3 was a little bit lower than the normal component of the nominal yield strength of the BRB, and this inadequacy was further amplified by the strain hardening of the BRB. As a result, obvious separation of the gusset plate can be observed in Figure 16(a). For the gusset plate in Specimen No.4, to which no pre-stress was provided, the tensile displacement was generally greater than that of Specimen No.3 even if the strut between the gusset plate the column on the other side carried part of the tensile force. After the 1/33 loading cycle of Specimen No.4, the strut was removed and another 1/33 loading cycle was conducted to verify the effect of the strut. As can be seen in Figure 16(b), the maximum displacement increased from about 0.4 mm to about 0.6 mm, about 50% increase, after removing the strut. Nevertheless, the normal displacement of the gusset plate was generally too small to be able to considerably influence the performance of the BRBs, no matter the pre-stressing force was small or there was no strut to share the force.

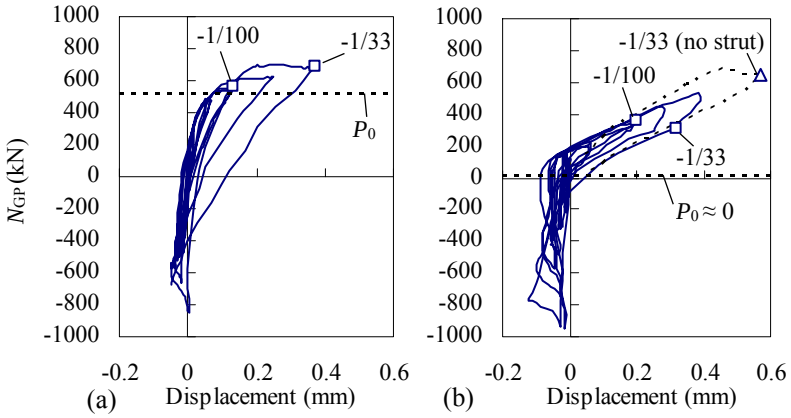

Figure 16. Relationship of force versus displacement of gusset plate normal to column surface: (a) Specimen No.3 and (b) No.4.

5.2 Shear response

The shear resistance of the gusset plate connection consists of both the resistance of the RC corbel, V_{corbel}, and the friction on the gusset plate-to-concrete interface, F_f (Figure 17). The friction force, F_f, is proportional to the difference between the total force in the bolts, denoted as T_B in Figure 17, and the normal force, N_{GP}, as shown in Figure 6, acting on the gusset plate by the BRBs (and by the strut for Specimen No.4) (Equation (2)). The shear deformation of the corbel was measured by two displacement transducers at the lower and upper toe of the gusset plate, that is, δ_L and δ_U in Figure 17. In the following discussions, the shear deformation of the gusset plate is taken as $(\delta_L-\delta_U)/2$, noting that the two transducers were installed in opposite directions.

$$F_f = \mu(T_B - N_{GP}) \tag{2}$$

where μ is the coefficient of friction.

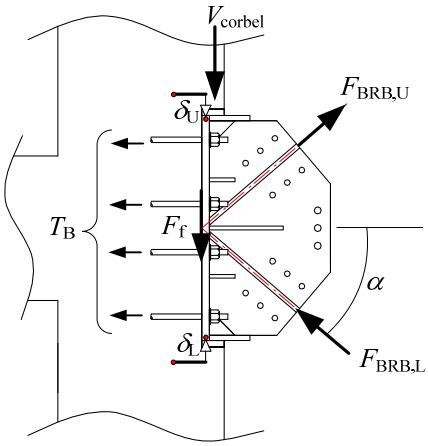

Figure 17. Force equilibrium of gusset plate during positive loading and measurement of gusset plate shear deformation.

Before the separation of the gusset plate, the force carried by a bolt keeps almost constant. Hence, the friction force, F_f, is greatly influenced by the normal force on the gusset

plate, N_{GP}. As can be seen in Figure 18, the friction force, F_f, in Specimen No.1 and No.2, assuming that the friction coefficient $\mu = 0.4$, was practically the same during positive and negative loading because the BRBs in the upper and the lower stories were identical or similar in strength and the normal force, N_{GP}, was thus small. For Specimen No.3 and No.4, however, obvious difference can be observed in the friction force, F_f, during positive and negative loading. For both specimens, the friction force, F_f, was much greater during the positive loading, when the normal force, N_{GP}, tended to push the gusset plate against the concrete, than during the negative loading, when N_{GP} tended to pull it away. In addition, the friction force in Specimen No.3 was much greater than in Specimen No.4 because of the large pre-stressing force in the bolts.

Because the friction force is highly dependent on the normal force, N_{GP}, and is likely to be much reduced or even completely eliminated (i.e., separation), it would be better to exclude its contribution to the shear resistance of the gusset plate connection in the design of such connections.

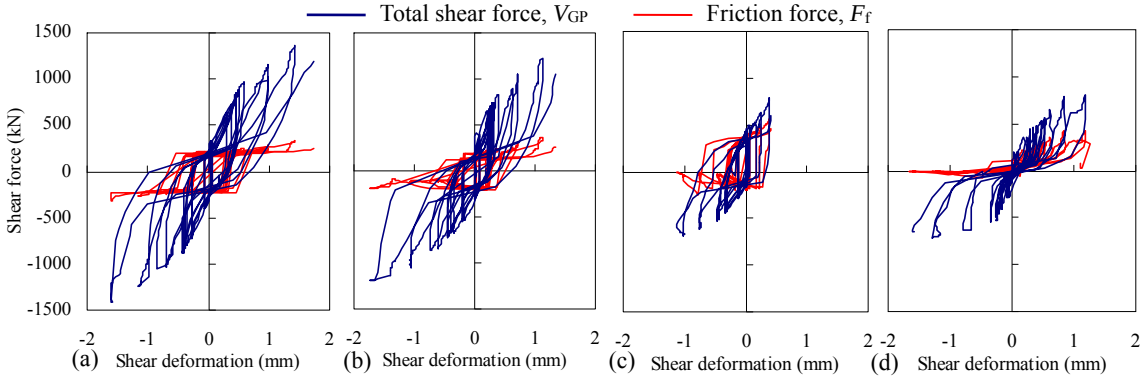

Figure 18. Shear resistance of gusset plate connection: (a) Specimen No.1, (b) No.2, (c) No.3 and (d) No.4.

With the assumed coefficient of friction, the shear force carried by the RC corbel, V_{corbel}, can be separated from the total shear force, V_{GP}. Take Specimen No.1 for example, whose corbels were subjected to the greatest shear force among the others. Figure 19 compares the shear force versus displacement relationship of both its corbels in the subassemblage test and the one in the lower story in a component test, which was conducted after the subassemblage test to obtain the shear strength of the corbel. The corbel failed in a very brittle manner in the component test at shear force 1061 kN, which was very close to the estimated shear strength in the design of the specimen. In the subassemblage test, the strain hardening of the BRBs exposed the corbels to greater than expected shear force and made the corbels, in Specimen No.1 in particular, very close to failure. This close-to-failure state was also confirmed by the strains in the corbel stirrups, which increased rapidly in the 1/33 loading cycle of Specimen No.1 in the subassemblage test, and was very close to those in the component test when the corbel was about to fail (Figure 20).

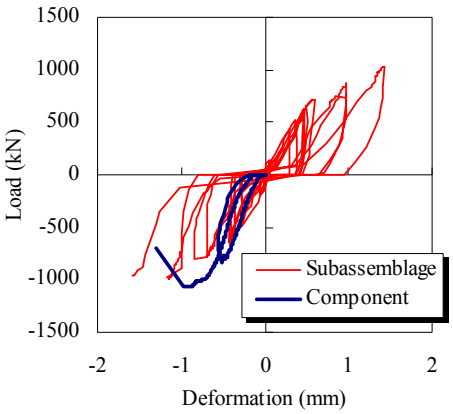

Figure 19. Corbel shear versus deformation relationship of Specimen No.1.

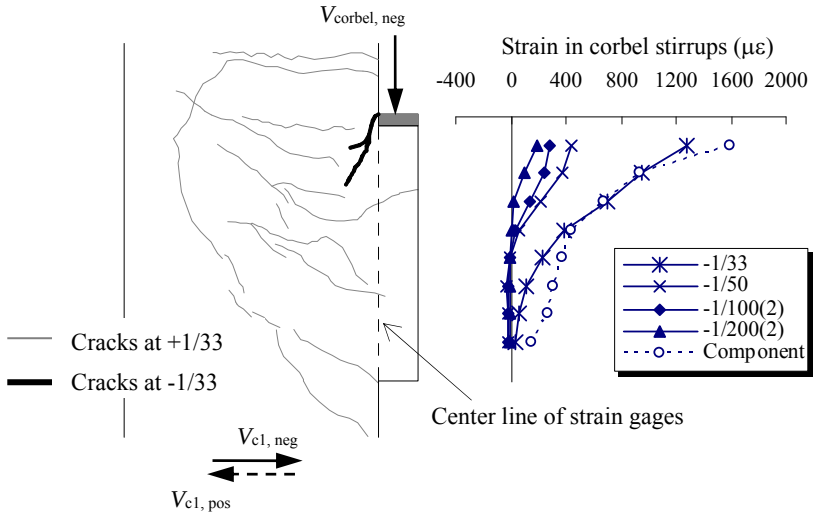

Figure 20. Cracks and stirrup strains of lower-story corbel of Specimen No.1.

On the other hand, by comparing the responses of the corbel in the subassemblage test and those in the component test, the bending of the underneath column seems to have little effect on the shear resistance of the corbel projecting from it. Again, take the lower corbel in Specimen No.1 for example. The corbel and its underneath column were bent and sustained some flexural cracks at the peak of a positive loading half-cycle (Figure 20), at which the corbel carried no shear force. In the consequent loading towards the negative direction, the BRBs may yield in the opposite direction much earlier than the RC part is fully unloaded. In other words, the lower corbel begins to carry great shear force, e.g., $V_{corbel,neg}$ in Figure 20, while the underneath column is still carrying shear force in the positive direction, e.g., $V_{c1,pos}$ in Figure 20, and thus may sustain some flexural cracking. However, these flexural cracks are generally perpendicular to the principal compressive stress because of the shear force $V_{corbel,neg}$, and thus are not likely to degrade the shear resistance of the corbel.

6. Conclusions

In order to verify the performance of the connection details for BRBs in an innovative continuously buckling restrained braced frame (CBRBF) system, a series of subassemblage

cyclic loading test were carried out. The following conclusions may be drawn from the above test observations and discussions.

(1) The BRBs generally yielded at about 1/600~1/500 story drift ratio before any considerable damage to the RC structure could be observed, and began to dissipate energy by stable plastic deformation.

(2) Because the BRB is connected to the gusset plate by bolted splice plates rather than ideal pins, plastic rotation may arise at the ends of the BRB. In the test, the observed end rotations were very close in magnitude to the story drift angle of the system. Nevertheless, the BRBs in the test performed well, despite the plastic rotation at the ends.

(3) As confirmed by the test, the vertical component of the great force in the BRBs, which is transmitted to the RC structure through corbels, helps increasing the moment resisting capacity of the frame, suppresses flexural cracking in the column segments under the corbels, but at the same time subjects the column in the lower story to additional unfavorable tensile force.

(4) While an RC corbel is resisting great shear force, it may at the same time prevent the gusset plate from being pulled away from the beam-to-column joint through friction, and thus make the gusset plate rotate with respect to the joint. This rotation may subject some of the bolts to greater force while some others to less force. This effect should be taken into account in the design of the bolt group, or otherwise, the friction between the corbel and the gusset plate should be eliminated.

(5) Both higher pre-stressing force in the bolts and a strut between the gusset plate and the column on the other side of the span would help reducing the normal displacement of the gusset plate. Nevertheless, this deformation is generally negligible even if the pre-stress is small and/or there is no strut.

(6) The behavior of the corbel is not much influenced by the deformation and damage of the underneath column. The performance of the corbel can be evaluated through simple component test.

The above observations generally show the validity of the proposed connection detail in a CBRBF system. It also lays a foundation for further investigation into the dynamic response of the CBRBF system to earthquake excitations, which is necessary to verify the global performance of the new buckling restrained braced system, to identify its response characteristics, and to evaluate the influence of the connection behavior.

Acknowledgments

This research investigation is funded by the Grants-in-Aid for Scientific Research (A) (22246090). This financial support is gratefully acknowledged. The authors are also grateful to the research team of Kumagai Gumi Co., Ltd. for their help in preparing and conducting the component test.

Reference

1. Fujimoto M, Wada A, Saeki E, et al. A study on brace enclosed in buckling-restraining mortar and steel tube. *Summaries of Technical Papers of AIJ Annual Meeting*, 1988: 1339-1342 (in Japanese).

2. Wada A; Nakashima M. From infancy to maturity of buckling restrained braces research. *Proc. 13th World*

Conference on Earthquake Engineering, 2004, in CD-ROM, Paper No. 1732.

3. Brown AP, Aiken ID, Jafarzadeh FJ. Buckling restrained braces provide the key to the seismic retrofit of the Wallace F. Bennett Federal Building. *Modern Steel Construction*, Aug, 2001.
4. Kukita S, Haginoya M, Miyagawa K, et al. Experimental Study on Seismic Retrofit for Existing R/C Building by using CHS Bracing. *Summaries of technical papers of AIJ annual meeting*, 2000, C-2: 377-382(in Japanese).
5. Ishii T, Mukai T, Kitamura H, et al. Seismic retrofit for existing R/C building using energy dissipative braces. *Proc. 13th World Conference on Earthquake Engineering*, 2004, in CD-ROM, Paper No.1209.
6. Yokouchi H, Kitajima K, Nakanishi M, et al. Experimental study on retrofit effect of an existing R/C school building retrofitted with energy dissipation devices. *Journal of Structural and Construction Engineering, Transaction of AIJ*, 2005, 592: 145-152 (in Japanese).
7. Mazzolani FM, Corte GD, D'Aniello M. Experimental analysis of steel dissipative bracing systems for seismic upgrading. *Journal of Civil Engineering and Management*, 2009, **15**(1): 7-19.
8. Ogawa Y, Isoda K, Kitamura Y, et al. Experimental study on the structural properties of high strength reinforced concrete frames with brace dampers. *Summaries of Technical Papers of AIJ Annual Meeting, 2004*: 1227-1230 (in Japanese).
9. Gu LZ, Gao XY, Xu JW, et al. Research on seismic performance of BRB concrete frames. *Journal of Building Structures*, 2011, **32**(7): 101-111 (in Chinese).
10. Sarno LD, Manfredi G. Seismic retrofitting with buckling restrained braces: Application to an existing non-ductile RC framed building. *Soil Dynamics and Earthquake Engineering*, 2010, **30**(11): 1279-1297.
11. Oviedo A JA, Midorikawa M, Asari T. Earthquake response of ten-story story-drift-controlled reinforced concrete frames with hysteretic dampers. *Engineering Structures*, 2010, **32**(6): 1735-1748.
12. AIJ. *Standard for structural calculation of reinforced concrete structures*. Architectural Institute of Japan, 2010 (in Japanese).
13. Qu Z, Maida Y, Kishiki S, Sakata H. Shear resistance of reinforced concrete corbels for shear keys. *Proc. 9th International Conference on Urban Earthquake Engineering*, Tokyo, Japan, 2012: 907-911.
14. BCJ. The building standard law of Japan, The Building Center of Japan, 2004 (in Japanese).
15. JSSI. *Manual for design and construction of seismically passive controlled building structures* (2nd Edition). The Japan Society of Seismic Isolation, 2007 (in Japanese).
16. Tsai KC, Hsiao PC. Pseudo-dynamic tests of a full-scale CFT/BRB frame - Part II: Seismic performance of buckling-restrained braces and connections. *Earthquake Engineering and Structural Dynamics*, 2008, **37**(7): 1099-1115.